ISSN 1070-3284, Russian Journal of Coordination Chemistry, 2019, Vol. 45, No. 8, pp. 539–547. © Pleiades Publishing, Ltd., 2019.
Russian Text © The Author(s), 2019, published in Koordinatsionnaya Khimiya, 2019, Vol. 45, No. 8, pp. 451–460.

Rhenium Tris(pyrazolyl)borate Oxothiolate Complexes: Syntheses and Structures

I. V. Skabitskii[a], *, S. G. Sakharov[a], A. A. Pasynskii[a], †, and R. S. Eshmakov[a]

[a] *Kurnakov Institute of General and Inorganic Chemistry, Russian Academy of Sciences, Moscow, 119991 Russia*

**e-mail: skabitskiy@gmail.com*

Received January 21, 2019; revised March 12, 2019; accepted March 14, 2019

Abstract—The rhenium complexes TpReOCl(S^{t}Bu) (**I**), TpReO(S^{t}Bu)$_2$ (**II**), and TpReO(S^{n}C$_3$H$_7$)$_2$ (**III**) are synthesized using two methods by analogy to the known thiophenyl complexes. Complexes **I**–**III** having more electron-donating alkylthiolate ligands are characterized by IR and NMR spectroscopy. The structures of complexes **I**–**III** are determined by X-ray diffraction analysis (CIF files CCDC nos. 1892096 (**I**), 1892097 (**II**), and 1892098 (**III**)). The temperature dependence of the spectra of the bis(thiolate) complexes allows one to determine the activation energy for the hindered rotation about the Re–thiolate ligand bond. The by-product of the reaction of TpReOCl$_2$ with NaS-*tert*-Bu, binuclear oxygen-bridged complex TpRe^{IV}Cl(S-*tert*-Bu)O(S-*tert*-Bu)$_2$Re^{IV}Tp, is isolated and structurally characterized (CIF file CCDC no. 1892099).

Keywords: rhenium complexes, thiolate complexes, tris(pyrazolyl)borate, hindered rotation, temperature-dependent NMR

DOI: 10.1134/S1070328419080086

INTRODUCTION

The tris(pyrazolyl)borate anion is a tridentate six-electron donor ligand forming stable complexes with rhenium. The anion is strongly bound to the metal and, hence, is not involved in ligand exchange reactions, is not oxidized, and is not reduced even under fairly drastic conditions. The tris(pyrazolyl)borate complexes behave, to a considerable extent, as analogs of the pentamethylcyclopentadienyl complexes. In particular, TpReOCl$_2$ (Tp is HB(C$_3$H$_3$N$_2$)$_3$) [1] by steric and electronic characteristics resembles C$_5$Me$_5$ReOCl$_2$ synthesized in situ by the reaction of Cp'ReCl$_4$ with water [2]. The TpReOCl$_2$ complex can be obtained directly from ammonium perrhenate on reflux in alcohol in the presence of hydrochloric acid (blue crystalline powder, IR spectrum: Re–O and B–H at 978 and 2528 cm^{-1}, respectively [3]).

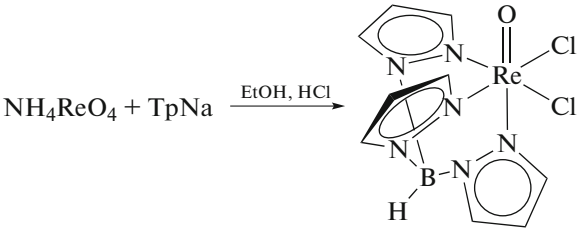

Chlorine atoms are readily substituted by thiolate groups in the reactions with thiols in the presence of bases. For example, the TpReO(SC$_2$H$_4$S) chelate complex with the strongly shortened Re=O bond (1.69 Å) was synthesized by the reaction of TpReOCl$_2$ with HSC$_2$H$_4$SH in the presence of triethylamine [4]. The compounds with one and two phenyl- and ethylthiolate ligands were obtained similarly. The consecutive substitution of the chloride ligands by one and two phenylthiolates results in the shift of the vibration band of the Re–O bond in the IR spectra of the complexes (978, 956, and 945 cm^{-1}, respectively) [5].

† Deceased.

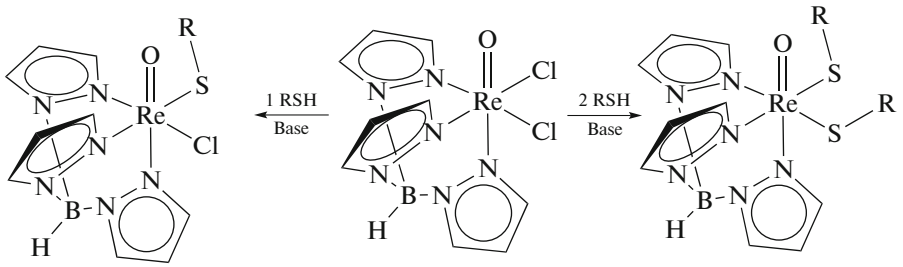

R = C_6H_5, CH_3CH_2 R = C_6H_5, CH_3CH_2, 2-Py

The purpose of this work is the synthesis of the rhenium tris(pyrazolyl)borate oxo-*tert*-butylthiolate complexes as promising metal-containing ligands for the preparation of heterometallic complexes in which the *tert*-butylthiolate groups provide a higher solubility and an easier thermal decomposition of the complexes during the production of nanosized inorganic compositions.

EXPERIMENTAL

Commercial ammonium perrhenate, *tert*-butylmercaptan, and di-*tert*-butyl disulfide (Acros organics) were used as received. The syntheses of $TpReOCl_2$ [1] and TpNa [6] were carried out according to described procedures. All procedures during the synthesis and isolation of products were conducted in anhydrous solvents under pure argon. Plates (MERCK) of silica gel 60 F254 on the aluminum basis were applied for thin-layer chromatography (TLC). IR spectra were recorded on a Bruker Alpha spectrometer using a Platinum ATR attachment. ^1H and ^{13}C NMR spectra were measured on a Bruker AV 400 instrument, and chemical shifts are presented relative to tetramethylsilane.

Synthesis of TpReOCl(S-*tert*-Bu) (I) and TpReO(S-*tert*-Bu)$_2$ (II). Procedure 1. Diazabicycloundecene (DBU) (80 μL, 0.54 mmol) and *tert*-butylmercaptan (50 μL, 0.44 mmol) were added to a suspension of $TpReOCl_2$ (100 mg, 0.21 mmol) in toluene (15 mL). The reaction mixture was stirred at 110°C in a sealed Schlenk flask for 24 h. Volatile components of the reaction mixture were removed in vacuo. The solid residue was dissolved in dichloromethane (10 mL), diluted with hexane (12 mL), and deposited on a chromatographic column (silica gel 14.5 × 1.5 cm), eluting the green and brown zones with a dichloromethane–hexane (1 : 1) system. The green eluate was evaporated to dryness, and the residue was dissolved in a mixture of dichloromethane (3 mL) and hexane (1.5 mL). The resulting mixture was kept at –25°C for 24 h. The precipitated green powder was filtered off, washed with pentane (4 times by 1.5 mL), and dried in vacuo. The yield was 53 mg (48%).

The brown fraction was evaporated to dryness, dissolved in heptane (1.5 mL), and kept at –25°C for 3 days. The precipitated crystalline aggregates were decanted, washed with pentane and cooled liquid nitrogen (4 times by 4 mL), and dried in vacuo. The yield was 13 mg (11%).

TpReOCl(S-*tert*-Bu): TLC (CH_2Cl_2): green spot, R_f 0.75; TpReO(S-*tert*-Bu)$_2$: TLC (CH_2Cl_2): yellow-brown spot R_f 0.67.

Synthesis of complexes I, II, and TpReCl(S-*tert*-Bu)O(S-*tert*-Bu)$_2$ReTp (IV). Procedure 2. Di-*tert*-butyl disulfide (1.1 mL, 5.7 mmol) and diglyme (0.5 mL) were added to a suspension of sodium (0.23 g, 10 mmol) in THF (20 mL). The reaction mixture was stirred for 24 h, and $TpReOCl_2$ (2.08 g, 4.3 mmol) was added to the obtained white suspension. The reaction mixture was heated at 65°C for 3 h. The solvent was removed in vacuo, and the obtained dark brown oil was extracted with heptane by portions of 60, 50, and 4 × 20 mL. The heptane extract was evaporated to 20 mL and chromatographed on a column packed with silica gel (3 × 15 cm). Three fractions were eluted: green (200 mL of a CH_2Cl_2–hexane (1 : 1) mixture), brown (250 mL of a CH_2Cl_2–hexane (1 : 1) mixture, and 50 mL of CH_2Cl_2), and violet (300 mL of CH_2Cl_2) fractions.

After the green fraction was evaporated in vacuo, a green powder of complex **I** was obtained in a yield of 65 mg (3%).

The brown fraction was evaporated to dryness, and the residue was dissolved in hexane (12 mL). The solution was kept at –25°C for 24 h. The precipitated thin needle-like crystals were filtered off at –70°C, washed with pentane cooled to the freezing onset (–130°C) in liquid nitrogen (3 times by 8 mL), and dried in vacuo. The yield of complex **II** was 327.6 mg (13%).

The violet fraction was evaporated to dryness, and the dark oil was extracted with hot hexane. The black-violet crystals of complex **IV** formed on keeping the extract at room temperature for 24 h were decanted, washed with hexane (3 × 5 mL), and dried in vacuo. The yield of complex **IV** was 1 mg (0.02%).

The residue that was not dissolved in heptane was extracted with benzene (40 mL). The obtained extract was kept at 5°C, and the formed brown precipitate was filtered off, washed with heptane (4 × 5 mL), and recrystallized from a mixture of dichloromethane

(10 mL) and hexane (10 mL). The obtained green powder was dissolved in CH_2Cl_2 (30 mL) and filtered through a silica gel layer. Hexane (5 mL) was added to the green solution, and the mixture was evaporated to dryness and dried in vacuo. The yield of complex **I** was 211.5 mg (9%).

Complex I: TLC (CH_2Cl_2): green spot, R_f 0.75. IR (ν, cm^{-1}): 3144 vw, 3119 vw br, 2954 vw br, 2915 vw br, 2856 vw, 2516 vw br, 1502 w, 1474 vw, 1453 vw, 1405 m, 1388 w, 1360 vw, 1310 m, 1211 m, 1186 w, 1165 w, 1116 m, 1073 vw, 1046 vs, 991 w, 958 vs, 919 vw, 890 vw, 863 vw, 816 vw, 792 w, 763 vs, 737 w, 710 s, 670 vw, 651 m, 613 m, 578 vw, 441 vw, 414 vw. ^{1}H NMR ($CDCl_3$), δ, ppm: 2.10 (s, 9H), 4.16 (br.m, 1H), 5.95 (dd, $^3J_{H-H}$ = 2.3 Hz, 1H), 6.45 (dd, $^3J_{H-H}$ = 2.3 Hz, 1H), 6.51 (dd, $^3J_{H-H}$ = 2.35 Hz, 1H), 7.31 (dd, $^3J_{H-H}$ = 2.35 Hz, 1H), 7.58 (dd, $^3J_{H-H}$ = 2.22 Hz, 1H), 7.79 (dd, $^4J_{H-H}$ = 0.60 Hz, $^3J_{H-H}$ = 2.35 Hz, 1H), 7.87 (dd, $^4J_{H-H}$ = 0.6 Hz, $^3J_{H-H}$ = 2.35 Hz, 1H), 8.17 (dd, $^3J_{H-H}$ = 2.2 Hz, 1H), 8.43 (dd, $^3J_{H-H}$ = 2.35 Hz, 1H). ^{13}C{^{1}H} NMR ($CDCl_3$), δ, ppm: 63.47; 34.50; 105.77; 107.53; 108.46; 132.68; 163.70; 139.16; 144.03; 145.93; 145.81.

Complex II: TLC (CH_2Cl_2): yellow-brown spot, R_f 0.67. IR (ν, cm^{-1}): 3108 vw br, 2954 w, 2915 w br, 2890 w, 2854 w, 2488 vw br, 1501 w, 1473 vw, 1453 w, 1406 m, 1390 m, 1358 w, 1309 m, 1217 m br, 1185 w, 1158 m, 1118 m, 1071 w, 1047 vs, 983 m, 936 vs, 890 w, 819 w, 794 w, 765 s, 756 s br, 713 s, 660 w, 617 m, 572 w, 439 w, 417 w. ^{1}H NMR ($CDCl_3$), δ, ppm: 1.67 (br.s, 18H), 4.47 br.m; 5.99 (dd, $^3J_{H-H}$ = 2.2 Hz, 1H), 6.40 (dd, $^3J_{H-H}$ = 2.3 Hz, 2H), 7.41 (dd, $^3J_{H-H}$ = 2.2 Hz, $^4J_{H-H}$ = 0.7 Hz), 7.70 (dd, $^3J_{H-H}$ = 2.4 Hz, $^4J_{H-H}$ < 0.4 Hz, 2H) 7.96 (dd, $^3J_{H-H}$ = 2.2 Hz, 1H), 8.38 (br.s, 2H). ^{13}C{^{1}H} NMR ($CDCl_3$), δ, ppm: 105.86; 107.10; 133.89; 136.78; 149.69; 145.67; 60.07; 34.34. ^{1}H NMR (toluene-d_8, 233 K), δ, ppm: 1.33 (s, 9H, S^t*Bu*), 2.41 (s, 9H, S^t*Bu*), 4.23 (br.m, 1B*H*); 5.40 (m, 1H), 5.66 (m, 1H), 5.71 (m, 1H), 7.01 (m, 1H), 8.10 (m, 1H), 8.15 (m, 1H), 8.64 (m, 1H).

Complex IV: TLC (CH_2Cl_2): violet spot, R_f 0.38. IR (ν, cm^{-1}): 3144 m br, 3101 m, 2952 m, 2910 m, 2884 m, 2851 m br, 2482 m br, 1499 m, 1469 w, 1451 w, 1403 s br, 1357 m, 1307 s, 1269 m, 1207 s br, 1153 s, 1117 s, 1098 m, 1069 m, 1043 vs, 983 s, 919 m, 887 m, 859 m, 838 m, 814 m, 788 m, 761 vs br, 733 s, 709 vs, 666 s, 648 s, 611 s, 574 m, 485 m, 436 m br.

Synthesis of complex III. Dipropyl disulfide (1.5 mL, 9.6 mmol) was added to a suspension of sodium (0.4 g, 17 mmol) in THF (20 mL). The reaction mixture was stirred for 24 h, and $TpReOCl_2$ (2.1 g, 4.3 mmol) was added to the obtained white suspension. The reaction mixture was stirred for 24 h, the solvent was removed in vacuo, and the obtained dark brown oil was extracted with benzene (60 mL). The benzene extract was poured onto a 10-cm column packed with silica gel and eluted with benzene (150 mL). The brown solution was evaporated to 30 mL, and heptane (30 mL) was added. The obtained solution was kept at 5°C, and the precipitated brown crystals were decanted, washed with hexane (3 times by 5 mL), and dried in vacuo. The yield of complex **III** was 1.3 g (53%).

The mother liquor was evaporated to dryness, and the residue was extracted with boiling heptane (4 times by 10 mL). The crystals of complex **III** precipitated on keeping the heptane extract at −25°C were decanted, washed with hexane (3 times by 5 mL), and dried in vacuo. The yield of complex **III** was 0.17 g (7%).

For $C_{15}H_{24}BN_6OS_2Re$ (*FW* = 566)

Anal. calcd., %	C, 31.86	H, 4.28	N, 14.86	S, 11.34
Found, %	C, 32.58	H, 4.56	N, 14.52	S, 11.18

IR (ν, cm^{-1}): 3146 vw, 3129 vw, 3109 vw, 2959 s, 2927 m, 2866 m, 2479 s, 1498 m, 1460 w, 1404 s, 1388 m, 1307 vs, 1222 m, 1205 s br, 1182 w, 1114 m, 1069 w, 1044 vs, 986 m, 938 s, 889 w, 854 vw, 814 vw, 789 w, 766 s, 711 m, 669 vw, 651 w, 614 w, 419 vs. ^{1}H NMR ($CDCl_3$, 298 K), δ, ppm: 1.06 (t, $^3J_{H-H}$ = 7.26 Hz, 6H, $SCH_2CH_2CH_3$), 1.91 (m, 4H, $SCH_2CH_2CH_3$), 2.97–5.04 (br.m, 5H, $SCH_2CH_2CH_3$ + B*H*), 5.94 (t, $^3J_{H-H}$ = 2.2 Hz, 1H), 6.43 (t, $^3J_{H-H}$ = 2.2 Hz, 2H), 7.37 (dd, $^3J_{H-H}$ = 2.2 Hz, $^4J_{H-H}$ = 0.8 Hz, 1H), 7.67 d, $^3J_{H-H}$ = 1.9 Hz, 2H), 7.79 (d, $^3J_{H-H}$ = 2.0 Hz, 1H), 8.32 (br.s, 2H). ^{13}C{^{1}H} NMR ($CDCl_3$, 298 K), δ, ppm: 14.1, 26.2, 45.5 v.br, 106.0, 107.4, 133.9, 136.8, 145.5, 147.9. ^{1}H NMR (toluene-d_8, 233 K), δ, ppm: 0.96 (t, $^3J_{H-H}$ = 7.10 Hz, 3H, $SCH_2CH_2CH_3$), 1.27 (t, $^3J_{H-H}$ = 7.0 Hz, 3H, $SCH_2CH_2CH_3$), 1.79 (m, 1H, $SCH_2CH_2CH_3$), 1.92 (m, 1H, $SCH_2CH_2CH_3$), 2.31 (m, 3H, $SCH_2CH_2CH_3$+ $SCH_2CH_2CH_3$), 3.45 (m, 1H, $SCH_2CH_2CH_3$), 4.25 (br.m, 1H, B*H*), 4.61 (m, 1H, $SCH_2CH_2CH_3$), 4.76 (m, 1H, $SCH_2CH_2CH_3$), 5.38 (t, $^3J_{H-H}$ = 2.1 Hz, 1H), 5.69 (br.s, 1H), 5.72 (br.s, 1H), 6.7 (d, $^3J_{H-H}$ = 1.7 Hz, 1H), 7.07 (br.m, 2H), 7.80 (m, 1H), 7.82 (br.s, 1H), 8.58 (br.s, 1H). ^{1}H NMR (toluene-d^8, 353 K), δ, ppm: 1.06 (t, $^3J_{H-H}$ = 7.20 Hz, 6H, $SCH_2CH_2CH_3$), 1.96 (m, 4H, $SCH_2CH_2CH_3$), 3.43 (br.s, 2H, $SCH_2CH_2CH_3$), 3.92 (br.m, 2H, $SCH_2CH_2CH_3$), 4.3 (br.m, 1H, B*H*), 5.51 (t, $^3J_{H-H}$ = 2.2 Hz, 1H), 5.88 (t, $^3J_{H-H}$ = 2.3 Hz, 2H), 6.89 (m, 1H), 7.27 (m, 2H), 7.77 (m, 1H), 8.20 (br.s, 2H). ^{13}C NMR (toluene-d_8, 353 K), δ, ppm: 14.2, 26.9, 45.9 br, 105.9, 107.2, 133.7, 136.6, 146.1, 148.5.

X-ray diffraction analysis was carried out on a Bruker APEX II CCD diffractometer. An absorption correction was applied by the method of multiple

Table 1. Crystallographic data and structure refinement parameters for complexes **I–IV**

Parameter	I	II	III	IV
Empirical formula	$C_{20}H_{27}BN_6OSClRe$	$C_{17}H_{28}BN_6OS_2Re$	$C_{15}H_{24}BN_6OS_2Re$	$C_{31}H_{47}B_2N_{12}OS_3Cl_3Re_2$
FW	631.99	593.58	565.53	1200.35
Radiation (λ , Å)		MoK_α (λ = 0.71073)		
Detection temperature, K	150(2)	150(2)	120(2)	150(2)
Crystal system	Triclinic	Monoclinic	Triclinic	Trigonal
Space group	$P\bar{1}$	*Cc*	$P\bar{1}$	$R\bar{3}$
a, Å	9.3684(8)	15.5182(4)	7.668(1)	27.782(1)
b, Å	11.177(1)	15.3550(3)	7.882(1)	27.782(1)
c, Å	12.715(1)	29.1704(6)	18.783(2)	29.663(2)
α, deg	111.161(1)	90	82.805(2)	90
β, deg	93.553(1)	92.9860(1)	82.007(2)	90
γ, deg	93.888(1)	90	65.269(2)	120
V, Å^3	1233.4(2)	6941.3(3)	1018.3(2)	19828(2)
Z	2	12	2	18
ρ_{calcd}, g cm^{-3}	1.702	1.704	1.844	1.809
μ, mm^{-1}	5.143	5.451	6.188	5.855
F(000)	620.0	3504.0	552.0	10 512.0
Scan range, deg	4.17–53.056	4.036–55.78	4.392–63.996	4.36–61.026
Scan mode		ω		
Independent reflections (N_1)	5087 (R_{int} = 0.0230)	16516 (R_{int} = 0.0419)	6683 (R_{int} = 0.0185)	13022 (R_{int} = 0.0458)
Reflections with $I > 2\sigma(I)$ (N_2)	4620	15726	6446	10254
Number of refined parameters	284	776	237	496
GOOF (F^2)	1.064	1.037	1.057	0.933
R_1 for N_2	0.0296	0.268	0.0171	0.0248
wR_2 for N_1	0.0740	0.423	0.0391	0.0543
$\Delta\rho_{max}/\Delta\rho_{min}$, e Å^{-3}	5.21/–0.98	0.91/–0.85	1.06/–1.12	2.14/–1.46

measurements of equivalent reflections using the SADABS program [7]. The structures of complexes **I–IV** were determined by a direct method and refined by least squares relative to F^2 in the anisotropic approximation of non-hydrogen atoms using the SHELX-2014 [8] and OLEX2 [9] program packages. The positions of hydrogen atoms were calculated geometrically. The crystallographic data and structure refinement parameters for compounds **I–IV** are presented in Table 1. Selected bond lengths and bond angles in complexes **I–IV** are given in captions to Figs. 1–4. The coordinates of atoms and other parameters for the structures of complexes **I–IV** were deposited with the Cambridge Crystallographic Data Centre (CIF files CCDC nos. 1892096–1892099; http://www.ccdc. cam.ac.uk/data_request/cif).

Quantum chemical calculations were performed in the framework of the density functional theory (DFT) using the ORCA 4.01 program package [10]. The geometry optimization of the complexes and transition states was carried out using the PBE functional [11, 12] with the double-split all-electron def2-SVP basis set [13] and the D3BJ empirical correction to dispersion interactions [14, 15]. The activation energy was calculated using the PBE0 hybrid functional [16] with the triple-split all-electron def2-TZVP basis set [13].

RESULTS AND DISCUSSION

Complexes **I** and **II** were synthesized using two different procedures. The first synthesis was carried out

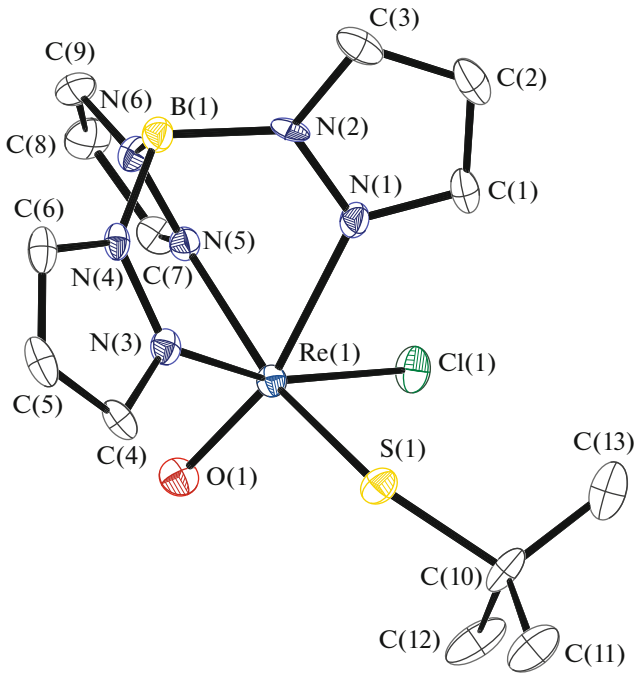

Fig. 1. Molecular structure of complex **I** (solvate toluene molecule is omitted). Selected bond lengths and bond angles: Re(1)–Cl(1) 2.355(1), Re(1)–S(1) 2.300(1), Re(1)–O(1) 1.686(4), Re(1)–N(1) 2.101(4), Re(1)–N(3) 2.165(4), Re(1)–N(5) 2.250(4), and S(1)–C(10) 1.861(5) Å; S(1)Re(1)Cl(1) 96.89(4)°, O(1)Re(1)Cl(1) 101.5(1)°, O(1)Re(1)S(1) 104.7(1)°, O(1)Re(1)N(1) 93.6(2)°, O(1)Re(1)N(3) 89.6(2)°, O(1)Re(1)N(5) 164.4(2)°, and C(10)S(1)Re(1) 119.9(2)°.

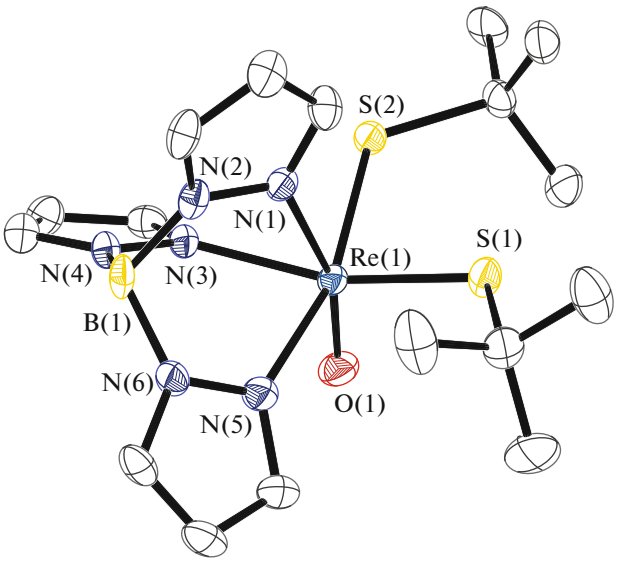

Fig. 2. Molecular structure of complex **II** (one of three independent molecules is shown). Bond lengths and bond angles: Re(1)–S(2) 2.310(2), Re(1)–S(1) 2.311(2), Re(1)–O(1) 1.682(4), Re(1)–N(3) 2.143(5), Re(1)–N(1) 2.261(5), Re(1)–N(5) 2.192(5), S(2)–C(14) 1.857(6), and S(3)–C(27) 1.859(6) Å; C(14)S(2)Re(1) 122.8(2)°, C(10)S(1)Re(1) 120.1(2)°, O(1)Re(1)S(1)C(10) 95.9(3)°, and O(1)Re(1)S(2)C(14) –83.3(3)°.

similarly to those for TpReOCl(SPh) and $TpReO(SPh)_2$ [5] by the reaction of $TpReOCl_2$ with *tert*-butylmercaptan in the presence of DBU as a base in toluene at 110°C. The reaction course was monitored by TLC on Silufol in dichloromethane from the disappearance of the blue spot of the initial $TpReOCl_2$ and the appearance of green (R_f 0.75) and yellow-brown (R_f 0.67) spots observed for the aforementioned phenylthiolate complexes [5]. The products were separated chromatographically and crystallized from a CH_2Cl_2–hexane (1 : 1) mixture for complex **I** and from hexane for complex **II**. The crystals of complex **I** suitable for X-ray diffraction analysis were obtained by keeping a toluene solution of complex **I** at –70°C.

The reaction of $TpReOCl_2$ with sodium *tert*-butylthiolate, which was obtained in THF from sodium and bis(*tert*-butyl disulfide) and used without isolation, was carried out according to procedure 2.

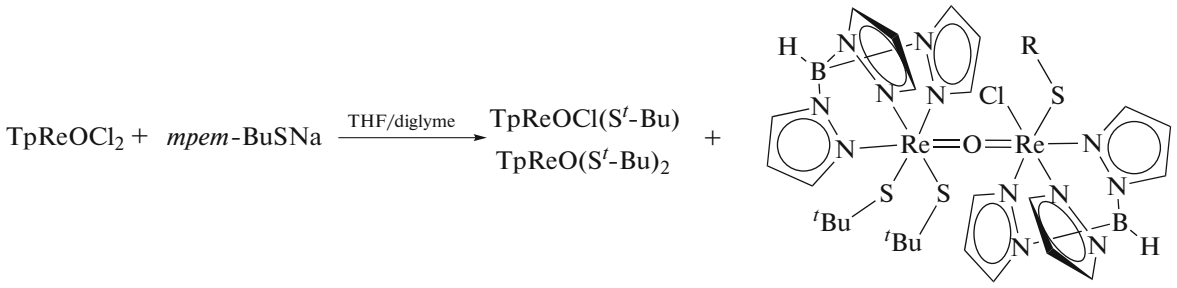

This reaction is faster than the reaction with mercaptan, but the monosubstituted product is also formed together with the disubstituted product in spite of the use of a 20% excess of *tert*-BuSNa. The reaction products were separated chromatographically, and a minor amount of new violet binuclear complex **IV** was isolated in addition to the mono- and dithiolate complexes. Complex **IV** was characterized by X-ray diffraction analysis, IR spectroscopy, and TLC (violet spot, R_f 0.38).

Propylthiolate complex **III** analogous to complex **II** was synthesized by the second method

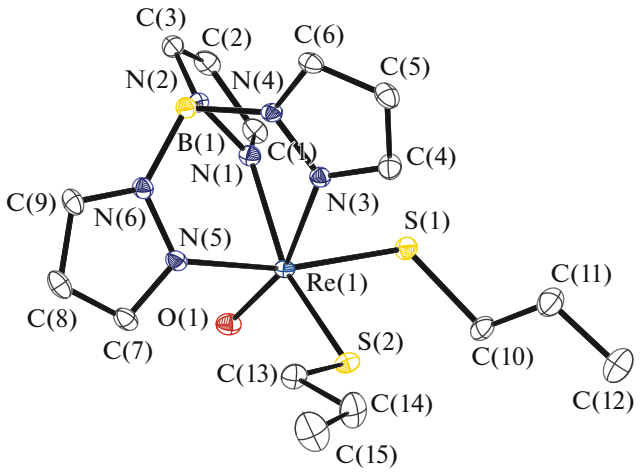

Fig. 3. Molecular structure of complex **III**. Bond lengths and bond angles: Re(1)–S(1) 2.3045(5), Re(1)–S(2) 2.3018(5), Re(1)–O(1) 1.697(1), Re(1)–N(1) 2.143(2), Re(1)–N(3) 2.268(2), Re(1)–N(5) 2.175(2), and S(1)–C(10) 1.832(2) Å; C(10)S(1)Re(1) 115.63(7)°, C(13)-S(2)Re(1) 112.36(6)°, O(1)Re(1)S(1)C(10) 87.30(9)°, and O(1)Re(1)S(2)C(13) 98.92(9)°.

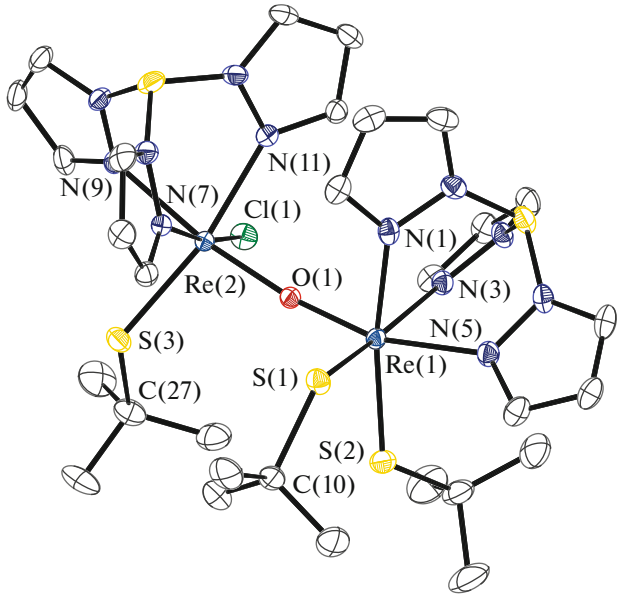

Fig. 4. Molecular structure of complex **IV** (solvated dichloromethane molecule is omitted). Bond lengths and bond angles: Re(1)–S(1) 2.3554(8), Re(1)–S(2) 2.2814(8), Re(1)–O(1) 1.8281(19), Re(1)–N(1) 2.160(3), Re(1)–N(3) 2.154(3), Re(1)–N(5) 2.171(2), Re(2)–Cl(1) 2.4048(8), Re(2)–S(3) 2.2742(8), Re(2)–O(1) 1.8842(19), Re(2)–N(7) 2.110(3), Re(2)–N(9) 2.139(2), and Re(2)–N(11) 2.145(2) Å; S(2)Re(1)S(1) 91.39(3)°, O(1)Re(1)S(1) 98.46(7)°, O(1)Re(1)S(2) 104.60(7)°, O(1)Re(1)N(1) 88.09(9)°, O(1)Re(1)N(3) 86.98(9)°, O(1)Re(1)N(5) 163.97(9)°, O(1)Re(2)Cl(1) 96.22(6)°, O(1)Re(2)S(3) 98.90(6)°, O(1)Re(2)N(7) 92.54(9)°, O(1)Re(2)N(9) 170.60(9)°, O(1)Re(2)N(11) 90.07(9)°, C(10)S(1)Re(1) 122.8(1)°, C(14)S(2)Re(1) 122.2(1)°, C(27)S(3)Re(2) 120.3(1)°, Re(1)O(1)Re(2) 170.2(1)°, O(1)Re(1)S(1)-C(10) 87.02°, O(1)Re(1)S(2)C(14) 108.25°, O(1)Re(2)-S(3)C(27) 71.33°, and N(7)Re(2)-Re(1)N(1) 56.95°.

using a twofold excess of $NaSC_3H_7$, which made it possible to avoid the formation of the monosubstituted complex.

The consecutive substitution of chloride substituents by more donating S-*tert*-Bu results in the shift of the band of Re=O vibrations (972, 958, and 936 cm^{-1}, respectively), indicating its weakening in the series **V**, **I**, **II**. The ^1H NMR spectra of complexes **II** and **III** are temperature-dependent. The signals of two nonequivalent thiolate groups and three nonequivalent pyrazole rings are observed at low temperatures, whereas at the high temperature the spectrum corresponds to equivalent thiolate groups and two of three equivalent pyrazole groups. This is most likely related to the hindered rotation about the Re–S bonds. The observed coalescence points of the signals of the pyrazole and thiolate groups (see, e.g., Fig. 5) make it possible to estimate the activation barrier for complexes **II** ($\Delta G^{\ddagger}_{259}$ = 13.03, $\Delta G^{\ddagger}_{281}$ = 12.97, $\Delta G^{\ddagger}_{291}$ = 13.06 kcal/mol) and **III** ($\Delta G^{\ddagger}_{278}$ = 12.6 kcal/mol). For *tert*-butyl complex **II**, the activation energy is almost temperature-independent, which assumes low activation entropy.

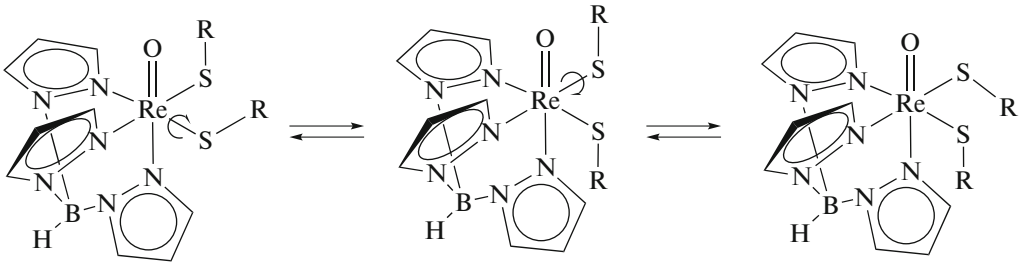

This indicates that the observed dynamic process is intramolecular and allows one to compare the determined free activation energies with the activation enthalpies obtained from the quantum chemical calculation.

The calculation of the barrier for this process by the DFT method gives activation energies of 12.3 and 14.1 kcal/mol for complexes **III** and **II**, respectively. The calculated Re–S distance in the transition state

for the rotating thiolate group is elongated to 2.47 Å compared to 2.31 Å for complex **III**, and the SReSC dihedral angle (104.5°) in the transition state does not correspond to the maximum of steric repulsion of any groups. This assumes that the rotation barrier in these complexes is mainly electronic in nature and is related to the substantial multiplicity of the Re–S bond. For complex **II**, the transition state for thiolate group rotation corresponds to the conformation in which the repulsion of the *tert*-butyl group and pyrazole fragment is maximum (SReSC 128.6°) and the elongation of the Re–S bond is less pronounced.

The structures of complexes **I–III** were determined by X-ray diffraction analysis. The Re–N distances in complex **I** are appreciably nonequivalent (2.25, 2.16, and 2.10 Å for bonds in the *trans* position to O, S-*tert*-Bu and Cl, respectively), most likely, because of differences in the *trans* effects of three different substituents. The short Re–O distance (1.686(4) Å) typical of similar compounds (Table 2) indicates triple bonding, as well as the OReS (104.7(1)°) and OReCl (101.5(1)°) angles strongly deviate from the octahedral angles. The Re–S bond length (2.300(1) Å) is noticeably shortened compared to the sum of covalent radii of Re and S (2.56 Å) [17]. This fact and the value of the CSRe angle (119.9(2)°), which is significantly larger than the ideal tetrahedral angle, suggest the multiple character of the Re–S bond according to the donation of the lone electron pair of the sulfur atom to the antibonding orbital of the triple Re–O bond. The conformation of the *tert*-butylthiolate ligand toward the chloride ligand (torsion angle OReSC 83.56°) is close to the screened conformation, which is also related, most likely, to this interaction.

In bis(thiolate) complex **II**, the Re–N distance in the *trans* position to oxygen (2.261(5) Å) is also noticeably longer than the distances in the *trans* position to the thiolate groups (2.143(2), 2.192(5) Å). The Re–S distances (2.310(2) and 2.311(2) Å) in complex **II** do not almost differ from the distance in complex **I**. This fact, along with the insignificant deviation of the *tert*-butyl groups from the ReS_2 plane and increased (over tetrahedral angles) ReSC angles (120.1(2)°, 122.8(2)°), indicates an appreciably multiple Re–S bond, which is the same as that in the monothiolate complex.

The replacement of *tert*-butyl substituents by *n*-propyl substituents in complex **III** does not almost change the geometry of the complex. A decrease in steric hindrances leads only to an insignificant additional shortening of the Re–S bonds (to 2.3045(5) and 2.3018(5) Å) and a decrease in the ReSC angles (115.63(7)°, 112.36(6)°). The conformation of the thiolate ligands remains almost unchanged.

Complex **IV** contains the dirhenium fragment Re=O=Re, and the Re–O distances in it (1.828(2) and 1.884(2) Å) are elongated over the terminal Re=O bond in the mononuclear complex (1.686(4) Å) but are noticeably shorter than the sum of covalent radii of Re and O (2.17 Å) [17]. Some deviation of the Re(1)O(1)Re(2) angle (170.2(1)°) from the rigidly linear value is related, most likely, to steric and packing effects of the *tert*-butylthiolate and tris(pyrazolyl)borate groups arranged in the *syn* position. The Re–N bonds with the nitrogen atoms in the *trans* position to the bridging oxygen atom (2.171(2) and 2.139(2) Å) are shortened compared to those in the monomer complex (Re–N 2.250(4) Å), most likely, due to a decrease in the *trans*-effect of bridging oxygen compared to the terminal one. A decrease in the order of the Re–O bond in the dimer is also indicated by a lower deviation of the O(1)Re(2)Cl(1) and O(1)-Re(2)S(3) angles (96.22(6)° and 98.90(6)°, respectively) compared to similar angles in TpReOCl(S-*tert*-Bu), (101.5(1)° and 104.7(1)°). The Re–S bonds (2.3554(8), 2.2814(8), 2.2742(8) Å) do not almost change, on the average, compared to those in the monomer complex and remain noticeably shortened. The ReSC angles close to 120° and the OReSC torsion angles (Table 3) also indicate a substantial contribution of the additional π-binding of the thiolate ligands with the Re atom.

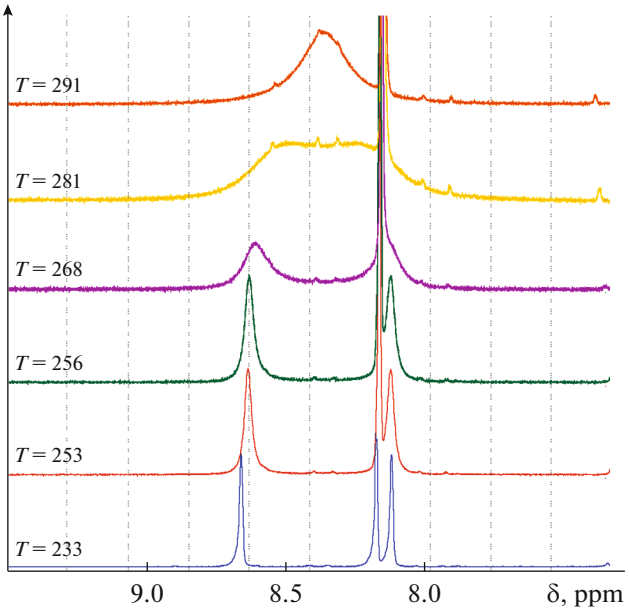

Fig. 5. Temperature dependence of the ^{1}H NMR spectrum of complex **II** in toluene-d_8.

A similar formation of the binuclear rhenium(III) oxo-bridged complex from the mononuclear fragments containing Re(IV) was observed in the reaction of $ReOCl_3(PPh_3)_2$ with the tetradentate ligand Tpa (tris(2-pyridylmethyl)amine) when eliminated triphenylphosphine acts as a reducing agent [20].

Table 2. Comparison of the structural and spectroscopic parameters of TpReOCl(S-*tert*-Bu) with the known analogs* and with $TpReOCl_2$

Compound	Torsion angle OReSC, deg	ν(Re–O), cm^{-1}	Re–O, Å	Re–S, Å	Literature
$TpReO(SC_2H_4S)$	96.79; 81.00	951	1.694(9)	2.280(4) 2.299(4)	[4, 5]
$TpReO(SC_2H_5)Cl$		961			[4]
$TpReO(SC_2H_5)_2$		932			[4]
TpReO(SPh)Cl	78.46	956	1.691(5)	2.301(2)	[5]
$TpReO(SPh)_2$	84.86; 95.12	945	1.668(5)	2.312(2); 2.310(2)	[5]
$TpReO(SC_6H_4S)$		952			[5]
$TpReO(SPy)_2$	93.23; 83.14	957	1.683(6)	2.317(2); 2.333(2)	[18]
$TpReOCl_2$		978			[5]
$TpReOS_2Fc$	89.64; 78.93	953	1.688(3)	2.316(1); 2.309(1)	[19]
TpReOCl(S-*tert*-Bu)	83.56	958	1.686(4)	2.300(1)	
$TpReO(S\text{-}tert\text{-}Bu)_2$	95.9(3) 83.3(3)	936	1.682(4)	2.310(2) 2.311(2)	
$TpReO(S\text{-}p\text{-}C_3H_7)_2$	87.30(9); 98.92(9)	938	1.697(1)	2.3045(5); 2.3018(5)	

* For analogs, see [4, 5, 18, 19].

Table 3. Comparison of selected structural parameters of $Tp_2Re_2OCl(S\text{-}tert\text{-}Bu)_3$ with the known analogs*

Compound	Angle ReORe, deg	Re(1)–O, Å	Re(2)–O, Å	Conformation	Literature
$[L'_2Re^{IV}_2Cl_2(\mu\text{-}O)][ZnCl_4]$ L' = 1,4,7-trimethyl-(1,4,7-triazo)cyclonane	180.0(1)	1.878(1)	1.878(1)	*anti*-	[21]
$[Re^{III}_2O(CH_3CN)_{10}]^{4+}$	180.000	1.7993(3)	1.7993(3)		[22]
$[Re^{III,IV}_2Cl_2O(Pa)_2]^{3+}$ Tpa = tris(2-pyridylmethyl)amine	178.0(1)	1.85(2)	1.84(2)	*anti*-	[20]
$Re^{V}_2(\mu\text{-}O)O_2Cl_2(BpaO_2)_2$ $BpaO_2$ = dipicolinoylamide	180	1.9122(1)	1.9122(1)	*anti*-	[23]
$Tp_2Re_2OCl(S\text{-}tert\text{-}Bu)_3$	170.17(12)	1.828(2)	1.884(2)	*syn*-	

* For analogs, see [11–14].

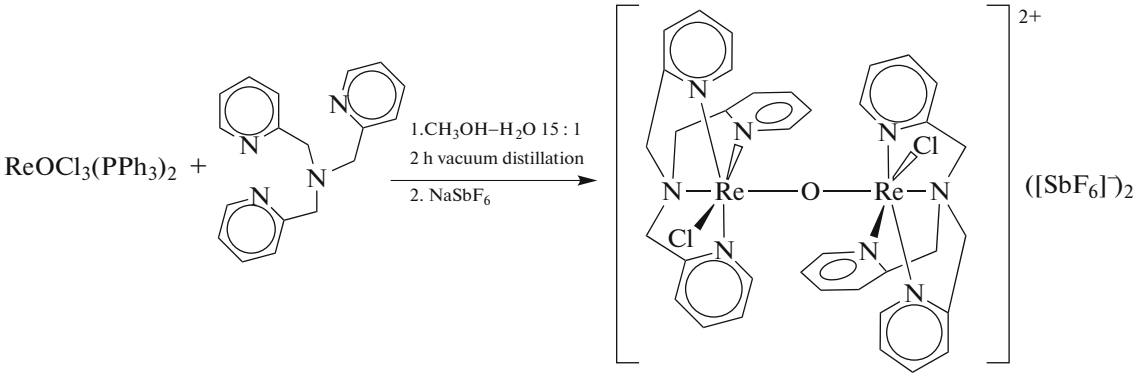

The main structural parameters of other known μ-oxorhenium complexes are presented in Table 3.

To conclude, the rhenium complexes TpReOCl(S-*tert*-Bu), TpReO(S-*tert*-Bu)$_2$, and TpReO(SC$_3$H$_7$)$_2$ with more electron-donating alkylthiolate ligands were synthesized using two methods by analogy to the known thiophenyl complexes. The new complexes were characterized by IR spectroscopy, NMR spectroscopy, and X-ray diffraction analysis. The study of the temperature dependence of the NMR spectra in combination with quantum chemical calculations suggests that in the dithiolate complexes rotation around the short (~2.3 Å) Re–S bonds is hindered with the barrier about 12.7 and 13.0 kcal/mol for the propylthiolate and *tert*-butylthiolate complexes, respectively. A weak dependence of the barrier on the alkyl substituent size and the elongation of the calculated Re–S distance in the transition state assume that the barrier is mainly electronic in nature and is related to a noticeably multiple character of the Re–S bond. The by-product of the reaction of TpReOCl$_2$ with NaS-*tert*-Bu, binuclear oxygen-bridged complex TpRe^{IV}Cl(S-*tert*-Bu)O(S-*tert*-Bu)$_2$Re^{IV}Tp, was also isolated and structurally characterized.

ACKNOWLEDGMENTS

The quantum chemical calculations were performed in the framework of the state task of the Kurnakov Institute of General and Inorganic Chemistry (Russian Academy of Sciences) in the sphere of basic research. The study was carried out using the equipment of the Center for Collective Use Physical Methods of Investigation at the Kurnakov Institute of General and Inorganic Chemistry (Russian Academy of Sciences).

FUNDING

This work was supported by the Russian Foundation for Basic Research (project no. 16-03-00798) and the Presidium of the Russian Academy of Sciences (program no. I.35.2.3).

CONFLICT OF INTEREST

The authors declare that they have no conflict of interest.

REFERENCES

1. Abrams, M.J., Davison, A., and Jones, A.G., *Inorg. Chim. Acta*, 1984, vol. 82, p. 125.
2. Cohen, E.A., McRae, G.A., Goldwhite, H., et al., *Inorg. Chem.*, 1987, vol. 26, p. 4000.
3. Brown, S.N. and Mayer, J.M., *Inorg. Chem.*, 1992, vol. 31, p. 4091.
4. Tisato, F., Bolzati, C., Duatti, A., et al., *Inorg. Chem.*, 1993, vol. 32, p. 2042.
5. Degnan, I.A., Behm, J., Cook, M.R., and Herrmann, W.A., *Inorg. Chem.*, 1991, vol. 30, p. 2165.
6. Trofimenko, S., Long, J.R., Nappier, T., and Shore, S.G., *Inorg. Synt.*, 1980, vol. 12, no. p. 99.
7. *SADABS (version 2008/1)*, Madison: Bruker AXS Inc., 2008.
8. Sheldrick, G.M., *Acta Crystallogr., Section A: Found. Crystallogr.*, 2008, vol. 64, p. 112.
9. Dolomanov, O.V., Bourhis, L.J., Gildea, R.J., et al., *J. Appl. Crystallogr.*, 2009, vol. 42, p. 339.
10. Neese, F., *WIREs Comput. Mol. Sci.*, 2018, vol. 8, p. e1327. https://doi.org/10.1002/wcms.1327
11. Perdew, J.P., Burke, K., and Ernzerhof, M., *Phys. Rev. Lett.*, 1996, vol. 77, p. 3865.
12. Perdew, J.P., Burke, K., and Ernzerhof, M., *Phys. Rev. Lett.*, 1997, vol. 78, p. 1396.
13. Weigend, F. and Ahlrichs, R., *Phys. Chem. Chem. Phys.*, 2005, vol. 7, p. 3297.
14. Grimme, S., Ehrlich, S., and Goerigk, L., *J. Comput. Chem.*, 2011, vol. 32, p. 1456.
15. Grimme, S., Antony, J., Ehrlich, S., and Krieg, H., *J. Chem. Phys.*, 2010, vol. 132, p. 154104.
16. Adamo, C. and Barone, V., *J. Chem. Phys.*, 1999, vol. 110, p. 6158.
17. Cordero, B., Gomez, V., Platero-Prats, A.E., et al., *Dalton Trans.*, 2008, vol. 21, p. 2832.
18. Kettler, P.B., Chang, Y.-D., Chen, Q., et al., *Inorg. Chim. Acta*, 1995, vol. 231, p. 13.
19. Herberhold, M., Jin, G.-X., and Milius, W., *J. Organomet. Chem.*, 1996, vol. 512, p. 111.
20. Sugimoto, H., Takahira, T., Yoshimura, T., et al., *Inorg. Chim. Acta*, 2002, vol. 337, p. 203.
21. Boehm, G., Wieghardt, K., Nuber, B., and Weiss, J., *Inorg. Chem.*, 1991, vol. 30, p. 3464.
22. Bera, J.K., Schelter, E.J., Patra, S.K., et al., *Dalton Trans.*, 2006, vol. 33, p. 4011.
23. Kochel, A. and Holynska, M., *Inorg. Chem. Commun.*, 2010, vol. 13, p. 782.

Translated by E. Yablonskaya